

Results of the Aerosol Sampling Experiment on the International Space Station

Marit E. Meyer¹

NASA Glenn Research Center, Cleveland, Ohio, 44135

The indoor air quality of the International Space Station (ISS), in terms of particulate matter, has been assessed through a sampling experiment that collected airborne debris for return to Earth. The Aerosol Sampling Experiment took place on ISS in December 2016 and January 2017, with sample return in February 2017. For redundancy, two different aerosol samplers collected particles in two size ranges spanning from 10 nm to hundreds of micrometers. Multiple analysis techniques have been used to characterize the particles, such as reflective light microscopy, manual scanning electron microscopy (SEM) analysis (secondary and backscattered imaging) with energy dispersive spectroscopy (EDS) x-ray analysis, and computer controlled scanning electron microscopy (CCSEM). Sampling took place in five locations on ISS, with the greatest deposition of particles in Node 3, followed by Node 1, the US Lab and Node 2. The Permanent Multipurpose Module (PMM) had very few airborne particles as it was a storage area having little human traffic. A large proportion of the sampled material consisted of fibers from clothing. Many particles had complex morphologies or contained multiple metals in a carbonaceous matrix. Metal particles were analyzed for each sampling location in terms of both weight and number percent, with 27 heavy metals detected. Fiberglass and TiO₂ particles were present in every location. Quantitative analysis results are presented, and where possible, particle emission sources are identified with the intention to fuel discussions on mitigation.

Nomenclature

<i>CCSEM</i>	=	computer controlled scanning electron microscopy
<i>COTS</i>	=	commercial-off-the-shelf
<i>EDS</i>	=	energy dispersive x-ray spectroscopy
<i>FE-SEM</i>	=	field emission scanning electron microscopy
<i>HEPA</i>	=	high efficiency particulate air
<i>HR-SEM</i>	=	high resolution scanning electron microscopy
<i>ISS</i>	=	International Space Station
<i>PAS</i>	=	Passive Aerosol Sampler
<i>PMM</i>	=	Permanent Multipurpose Module
<i>SDD</i>	=	silicon drift detector
<i>SEM</i>	=	scanning electron microscope
<i>STEM</i>	=	scanning transmission electron microscopy
<i>TEM</i>	=	transmission electron microscope

¹ Research Aerospace Engineer, Combustion Processes and Reacting Systems Branch, 21000 Brookpark Road Mailstop, Cleveland, Ohio 44135.

² Certain commercial equipment, instruments, or materials are identified in this paper to foster understanding. Such identification does not imply recommendation or endorsement by the National Aeronautics and Space Administration (NASA), nor does it imply that the materials or equipment identified are necessarily the best available for the purpose.

I. Introduction

THE quality of the air on a spacecraft has direct consequences for the health and wellbeing of the crew. The current mitigation technique for airborne particulate matter, or aerosols, in ISS air is HEPA filtration. This is generally successful, but since humans and equipment are sources of aerosols, there can be localized higher concentrations. On Earth, gravity causes larger particles to settle, so under normal circumstances, humans do not have to contend with particles on the order of $100\ \mu\text{m}$ in the breathing zone. In low gravity, however, particles of this size will remain airborne and follow the air flow patterns of the air handling system until they are deposited on air intake vents. Therefore, the Aerosol Sampling Experiment was designed to capture these larger particles by placing passive samplers above these vents in seven locations on ISS. Additional sampling by commercial-off-the-shelf (COTS) Active samplers collected particles in smaller size ranges. An overview of the sampling hardware and methodology is found in reference 1. The passive aerosol samplers (each designated PAS followed by a S/N letter) were on vents and filters which are normally keep-out zones, but exceptions were granted in order to obtain valuable information on the state of the air quality on ISS. Passive samplers were deployed in the U.S. Lab (2 locations), Node 1, Node 2, Node 3 (2 locations), and the Permanent Multipurpose Module (PMM) (Figure 1). Locations were chosen to capture particles during crew exercise, in the hygiene area, near a hatch opening from a visiting vehicle, and in a storage area (to compare particle numbers with locations with regular human traffic). Since a preliminary study on sampling times was not feasible on ISS, the passive sampler was designed with five separate sampling substrates that were exposed for different durations (2 days, 4 days, 8 days, 16 days and 32 days), with the expectation that one of the surfaces will have optimal particle coverage for microscopic analysis. Active samplers were deployed near most passive samplers for six hours to sample the same air at one point during the 36 day passive sampler deployments. An additional active sampler deployment was performed during crew exercise in two locations in Node 3 after the passive samplers were complete and stowed. The dates and locations of the particle sampling are given in Table 1.

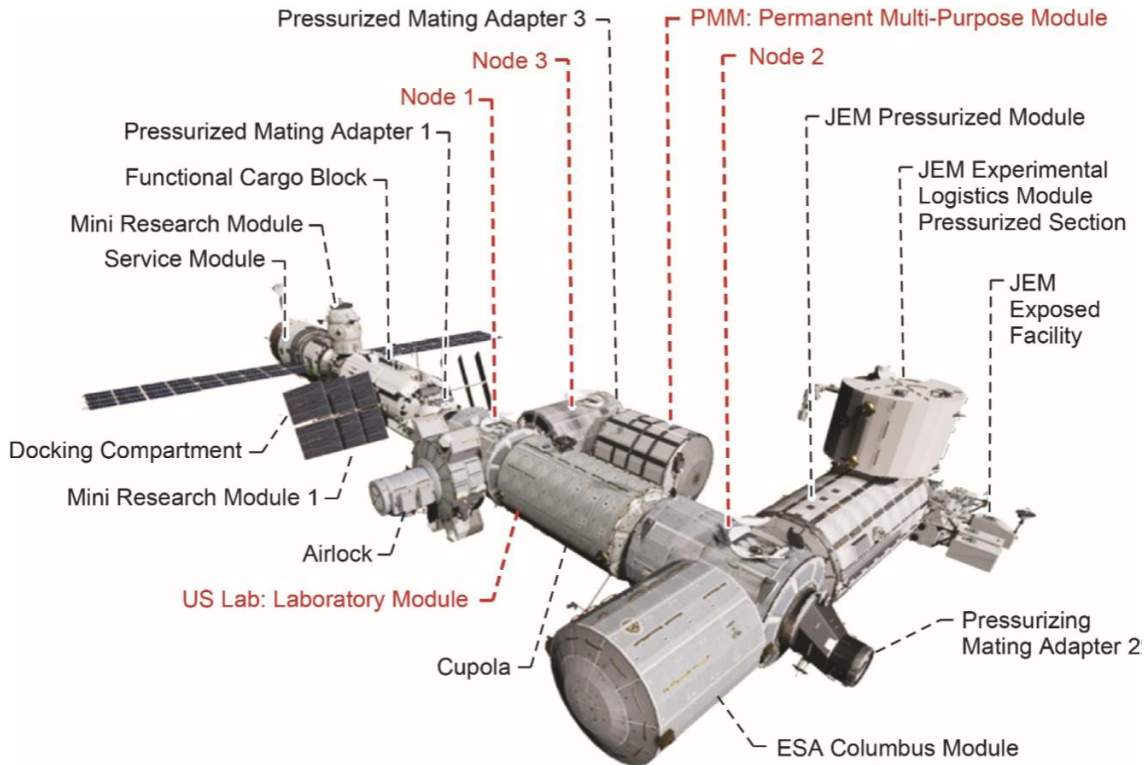


Figure 1. Sampling locations (in red) for the Aerosol Sampling Experiment on ISS

Table 1: Passive Sampler Locations and Co-located Active Sampling Sessions

Passive Sampler	Location	Relevant Activities	Date of Active Sampling
PAS B	Node 1 Deck 1	Eating Area	12/8/2016
PAS D	Node 3 Deck 3	Hygiene and Exercise	12/15/2016
PAS E	Permanent Multipurpose Module (PMM)	Storage Area	12/22/2016
PAS F	Node 2 Deck 2	Where vehicles dock	11/29/2016 and 12/15/2016
PAS G	Node 3 Forward 3	Hygiene and Exercise	11/29/2016
PAS J	US Lab Bay 1 Starboard Deck	Experiments	12/8/2016 and 12/22/2016
PAS K	US Lab Bay 3 Port/Deck Standoff	Experiments	N/A
Bonus	Node 3 OGS (Node3A5)	Hygiene and Exercise	1/18/2017
Bonus	Node 3 Bay 3 Overhead Midbay	Hygiene and Exercise	1/18/2017

II. Passive Sampler Results

Each of the 29 x 15 mm sampling substrates from the passive aerosol samplers were analyzed with a scanning electron microscope (SEM). A montage for each sample was created by combining fields of high resolution SEM backscattered electron images, which can be enlarged to the nanometer scale. These images can be analyzed subsequently without a microscope for manual and computer-controlled microscopy. A montage of the PAS K 16-day sample is shown in Figure 2 (a). Note that there are many fibers present, which creates difficulties for automated analysis of the montages. The edge detection algorithm for image software is confounded by the length of the fibers and the lack of contrast between fibers and some particle materials, particularly those with low atomic numbers. Brighter particles seen in the montage are occasionally individual metal particles, but more frequently, they are one of many pieces of metal embedded in the matrix of a larger particle. The visible portion of the metal part may or may not be representative of the full size of the metal piece, because a large volume could be hidden by the particle matrix material, in the same way the visible portion of an iceberg is not representative of its full volume of ice. Therefore, the metals size distribution results must be interpreted carefully, with the caveat that the particles detected and sized are only the visible portions of the metals present in the sample which contains large multi-component particles.

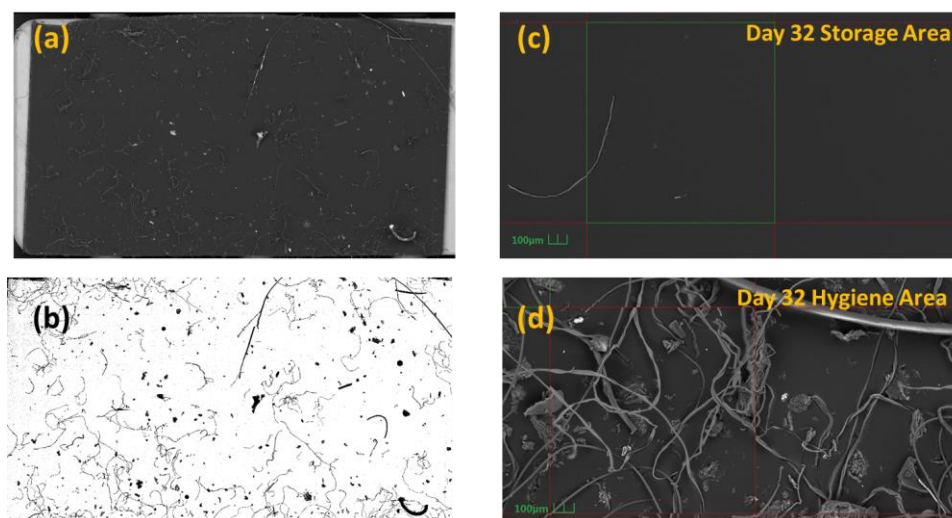


Figure 2. Example of particle coverage on PAS substrates: (a) is the PAS K 16-day montage of the 29 x 15 mm sampling substrate created by combining fields of high resolution SEM images, (b) is the binary (black/white) image of (a), analyzed with ImageJ software. The right images show a portion of the montages, enlarged with scale bar of 100 µm, comparing portions of the 32-day substrates from PAS E (PMM, storage area) (c) with PAS G (Node 3, exercise and hygiene area) (d).

To see the relative accumulation of airborne debris collected (including particles and fibers), the area fraction (percent) coverage of particles on each passive sampler substrate was calculated using ImageJ (Ref. 2). The montage image was uploaded into ImageJ, which is image analysis software in which the edge detection threshold was adjusted for particles brighter than the dark background (black carbon tape). This created a black and white (binary) representation of the sample as shown in Figure 2 (b), with the black representing particles and fibers present on the tape. Then the particle area fraction was calculated by taking the ratio of total dark area to the total area. Figure 3 shows the results of the sample collection, which demonstrates that particles were uniformly deposited over the different sampling durations. Also, the highest proportion of airborne particles are in Node 3 (hygiene and exercise area) on PAS G and D, followed by PAS B, which is in Node 1 where the crew eats. The least particles were sampled in the PMM storage area, on PAS E. This is the expected outcome, because locations where humans are engaged in vigorous activity will emit large amounts of particles emitted, and locations not frequented by humans (i.e., the PMM storage area) will have much fewer particle emission sources. Enlarged portions of the PAS G and PAS E montages are shown in Figure 2 (c) and (d), illustrating the vastly different airborne particle concentrations in the ‘cleanest’ and ‘dirtiest’ ISS locations.

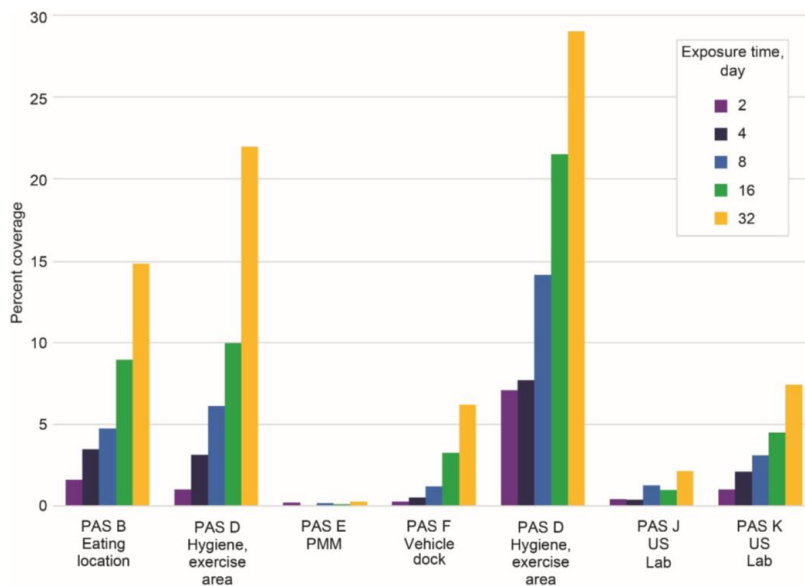


Figure 3. Percent of passive sampler substrate area covered with particles and fibers, based on ImageJ analysis (example of binary image is in Figure 2 (b)).

A. Metals Analysis

Computer-controlled SEM (CCSEM) was used to analyze metals present on the passive samples using energy dispersive x-ray spectroscopy (EDS), which identifies chemical elements present in the samples (molecular structure of these elements is not identified). Based on information obtained from the initial manual SEM review and the examination of the montage images, one sample from each of the seven passive sampler locations was selected for more detailed analysis using CCSEM analysis. The IntelliSEM software (RJ Lee Group, Monroeville, Pennsylvania) was used to scan the samples for particles greater than 1 μm containing high atomic number elements (titanium and greater). Unfortunately, this omits single-component aluminum particles and salts, which was a necessary restriction for accurate edge detection of individual particles. Aluminum is accounted for when it is present with other higher atomic number metals in the same particle. Individual aluminum and salt particles may be addressed in future analyses. Another limitation of the automated analysis was the presence of many types of fibers, which confuse edge detection algorithms, and also necessitated the selection of the element titanium as the minimum threshold for particle edge contrast. Upon detection by the software, particle diameter was measured at 45 different angles to get maximum, minimum, and average Feret diameters (in a fraction of a second), and an elemental spectrum was collected by EDS for 5 or 10 seconds, along with a digital image of the particle. Results were reviewed manually, and appropriate rules were created to classify separate particle types. Based on these rules, the software used a

sorting scheme to group particles into classes based on their elemental composition. A manual SEM review was performed to gain additional information on complex structures detected during the analysis. Over 27 metals with atomic number higher than titanium were found. Example results of a metal particle analysis is shown in Figure 4, from PAS G, which was in Node 3 (exercise and hygiene area).

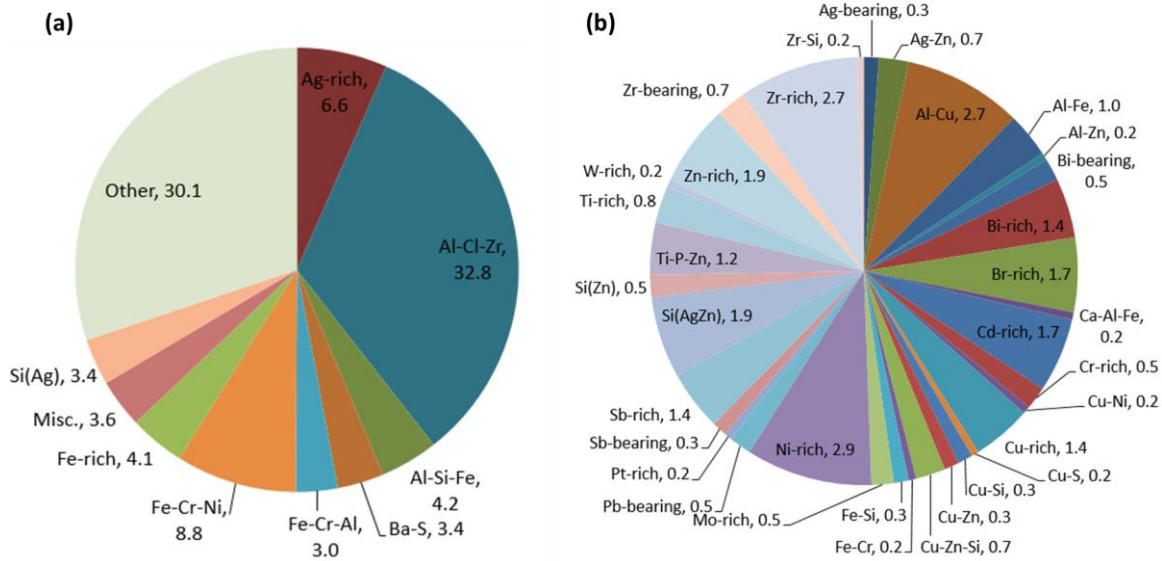


Figure 4. CCSEM results of PAS G, 8 day sample from Node 3 where crew exercise and hygiene take place. Percentages of total number concentrations of metal particles greater than 1 μm are shown where (a) shows overall results and (b) is the breakdown of particle material classes in category ‘Other, 30.1.’ Particles considered in this analysis are visible high-contrast metals which are typically not individual particles, but rather, metal pieces embedded in complex larger particles.

Different alloys can be identified in the material classes shown in Figure 4a, for example, stainless steel (Fe-Cr-Ni), Kanthal (Fe-Cr-Al), and 4006 aluminum alloy (Al-Si-Fe). Other alloying elements added to aluminum include Cu, Fe, Zn and Ca, all of which are represented in small percentages in the category ‘other’ (Figure 4b), covering particle classes that represent less than 3% of all particles analyzed.

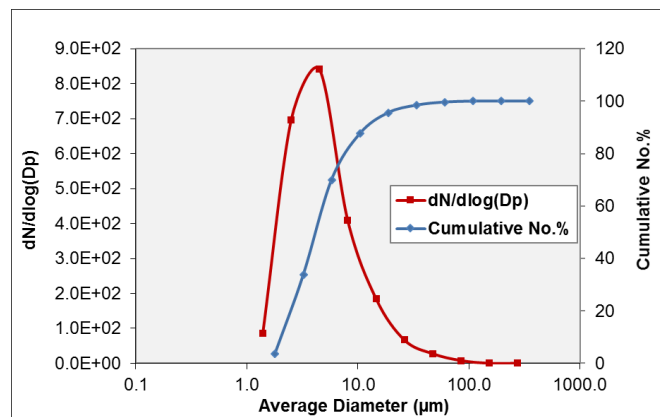


Figure 5. Particle size distribution from the CCSEM metals analysis for PAS G, 8-day sample. This is based on 590 metal particles greater than 1 μm detected, with maximum diameter 69.4 μm and average diameter 6.3 μm . Note that these may not be individual particles, but may be embedded within a carbon matrix of a larger particle.

The plotted size distribution of metal particles in the CCSEM analysis of Figure 4 is shown in Figure 5, which was based on 587 total particles counted, having a minimum diameter of 1 μm (which was a pre-established analysis parameter), maximum diameter of 69.4 μm , and average diameter of 6.3 μm . Note that these are not necessarily individual metal particles, but may be embedded in multi-component particles having a carbonaceous matrix.

A similar analysis was performed for all types of particles, including carbonaceous particles, for one PAS substrate from the US Lab (S/N K, day 16). The inclusion of carbon-rich particles necessitated the larger minimum particle size threshold of 5 μm . Based on 1306 particles counted, the maximum diameter was 556 μm and the average diameter was 35.6 μm . These sizes are not representative of the entire ISS aerosol population, as the passive sampler was designed to only capture larger particles. The majority of the particles were carbon-rich (70% by weight, 47% by number). Possible sources of these particles may be skin flakes, food, paper, and plastics, among other things. The breakdown of particle material classes by weight percent (a) and number percent (b) are shown in Figure 6.

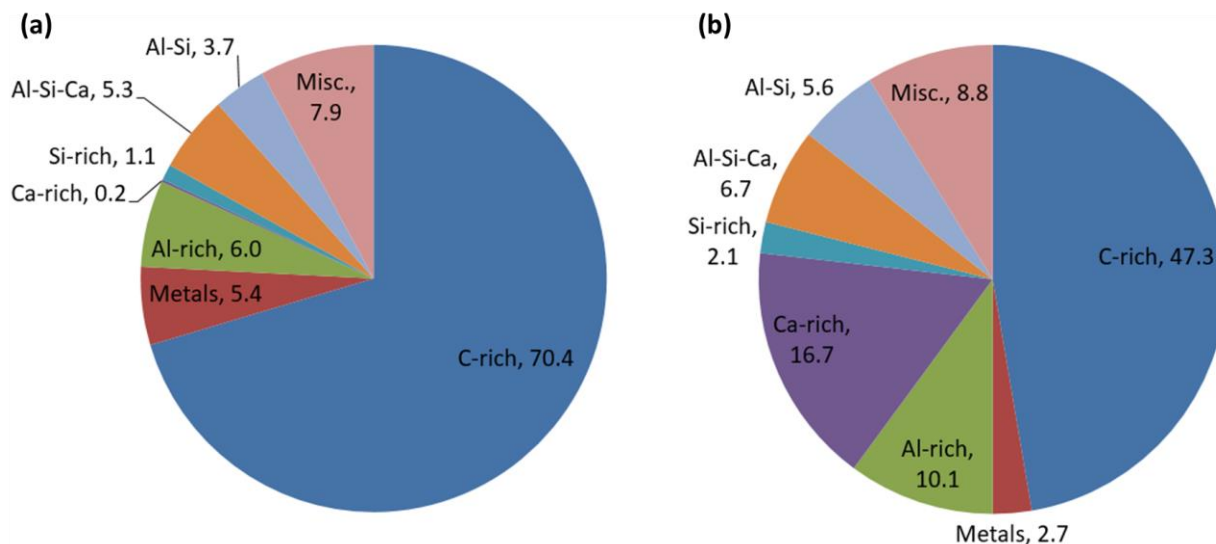


Figure 6. CCSEM results of PAS K, 16 day sample from the US Lab. Relative concentrations of all particles greater than 5 μm are shown. (a) shows the relative concentration by weight percent and (b) shows the relative concentration by number percent of particle material classes.

B. Particle Emission Sources

Ongoing research will investigate the classes of materials in the metals analyses, with the aim to identify, if possible, what the sources of the particles may be.

One example of a likely particle emission source can be deduced from the pie chart in Figure 4. The most abundant particle class (32.8% of all particles analyzed) on the PAS G sample in Figure 4 consists of the elements aluminum, chlorine, and zirconium. This is assumed to be the compound aluminum zirconium tetrachlorohydrate, which is a preparation used as an antiperspirant in deodorant products. This is a logical material in Node 3, where crew members exercise and do personal hygiene. Deodorant particles may be emitted during exercise, or while using wipes after exercising, in addition to the original application of the product. In the absence of laundry on ISS, the crew members wear clothing repeatedly, including exercise wear, before disposing of them in the trash. Thus, deodorant particles embedded in the fabric can be liberated and re-entrained into the cabin air when donning and doffing clothing. An example of a multi-component particle containing aluminum, chlorine, and zirconium is shown in Figure 7, where the particle is accompanied by three different spectra showing the elements present in different locations on the particle. The EDS area scan of the entire particle shows the elements Al, Cl, Zr, Si, Mg, Na, Cl, K, C and O. The middle EDS spectrum corresponds to the Al-Cl-Zr particle indicated in the blue outline, and the lower EDS spectrum shows a different Al-Cl-Zr particle which also has Si and Mg, elements in Talc

(chemical formula $H_2Mg_3(SiO_3)_4$ or $Mg_3Si_4O_{10}(OH)_2$). Talc is often a component of deodorant products. The presence of Na and Cl indicates salt (likely from human sweat), and the presence of potassium (element K) is indicative of human biology, as it is found in all human cells. Note that there are two lint fibers overlapping the particle, approximately 5 μm and 15 μm in diameter, respectively.

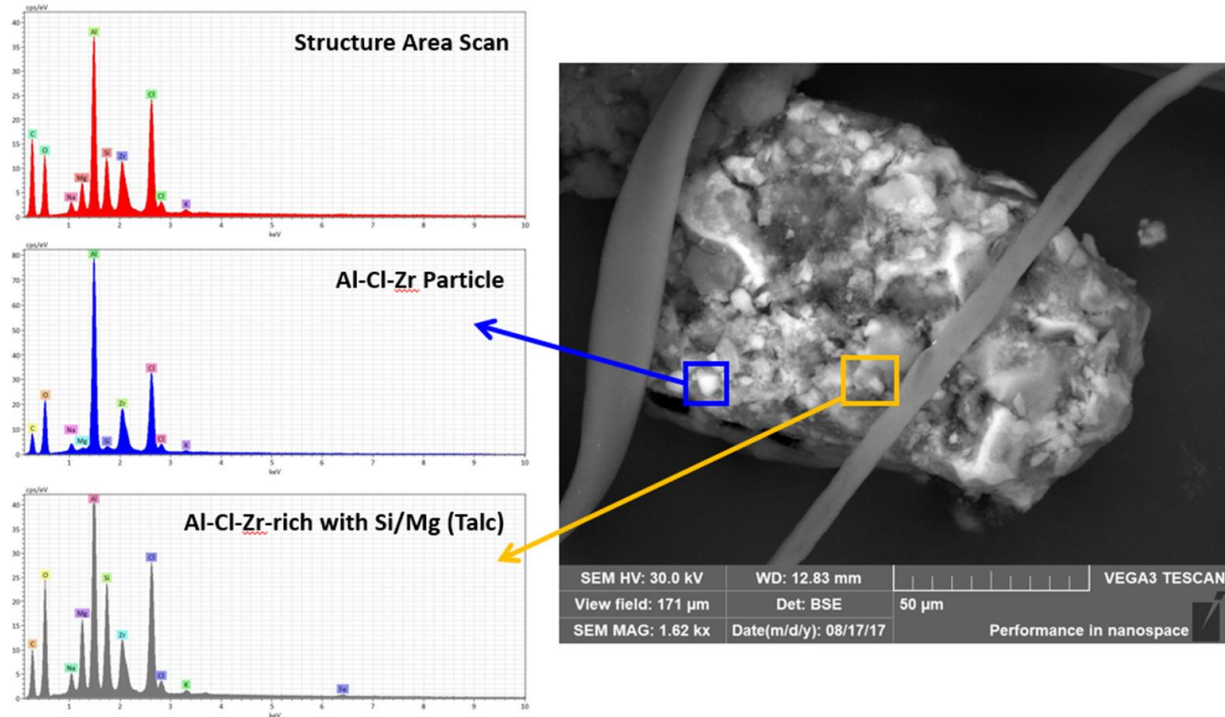


Figure 7. A complex agglomerated particle containing aluminum, chlorine, and zirconium, which is likely a preparation used as an antiperspirant in deodorant products. The upper spectrum is an EDS area scan of the entire particle. The middle spectrum corresponds to an individual Al-Cl-Zr particle, and the lower spectrum is different location which also has Si and Mg, ingredients in talc.

The second highest material category in Figure 4 is 8.8%, containing iron, chromium, and nickel, indicative of stainless steel, which likely comes from the mechanical abrasion of moving metal parts. While this material is ubiquitous on ISS, one likely source is exercise equipment. Both PAS D and G were in Node 3 where the Advanced Resistive Exercise Device (ARED)³ is located. Crew members exercise two hours per day, on average, with ARED used regularly over the passive sampling period. An example of a stainless steel wear particle from PAS D, collected near ARED, is shown in Figure 8, along with the EDS spectrum. The morphology is indicative of mechanical abrasion, as striations are visible, along with indications of brittle fracture. This particle is on the order of 100 μm (about the diameter of a human hair), and while it is not inhalable, as foreign object debris (FOD) it would be an eye hazard.

The vents drawing air from Node 3 capture metal particles such as the one in Figure 8, which become entrained in the flow. Future spacecraft design should apply the practice of placing air intakes near emission sources and design ventilation systems to capture FOD before it enters larger mixing flow fields in the cabin, thus reducing crew member exposure. This design practice requires understanding particle emissions of the different types of equipment and infrastructure in the spacecraft.

On Earth, these types of metal particles are removed from the air quickly by gravitational settling. If the particle in Figure 8 is approximated as equivalent to a 100 μm diameter sphere, a representative stainless steel particle from an exercise machine on Earth would settle from a height of 1 meter in roughly 0.5 seconds.

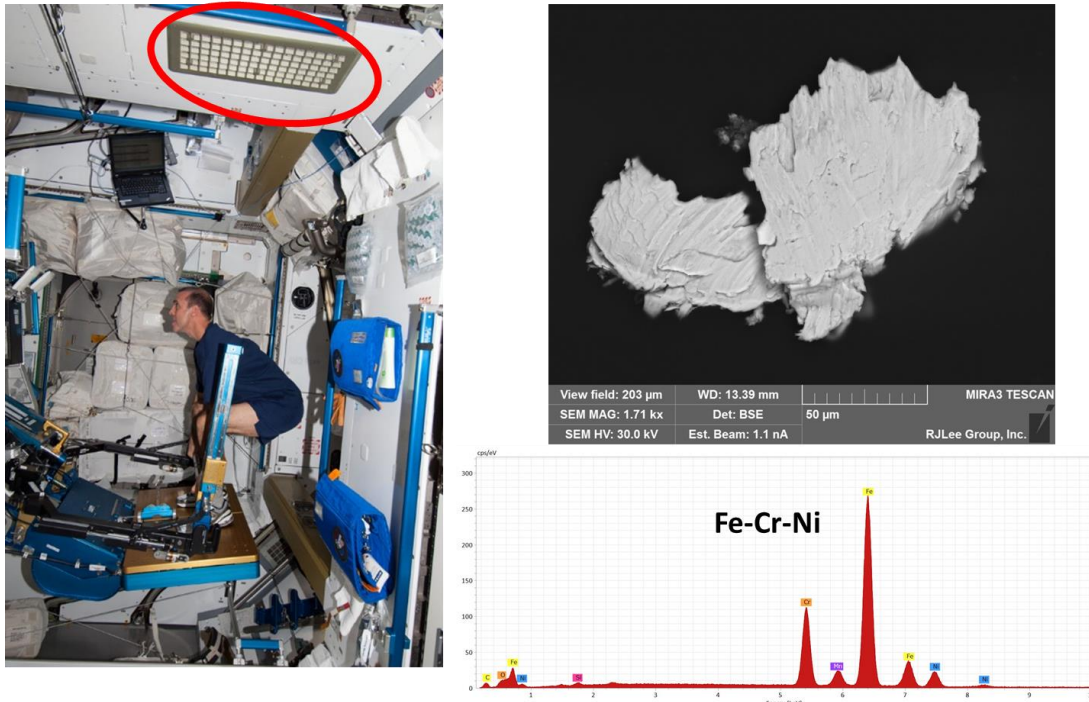


Figure 8. Advanced Resistive Exercise Device (ARED) is shown (left image) with the adjacent vent highlighted where PAS D captured the metal wear particle in the micrograph. The EDS spectrum of the particle shows iron, chromium and nickel, characteristic of stainless steel alloy.

An investigation into the materials that comprise ARED showed that a significant percent of the particles collected on Node 3 passive samplers can be attributed to this equipment.⁴ Figure 9 shows the metals analyses for PAS D and PAS G, indicating the percentages of the total weight of particles analyzed, with ARED materials shown in blue. Approximately 70% of metal particles (by weight) collected on PAS D were materials found in ARED, as were over 90% of all metal particles (by weight) on PAS G. The other significant particle material class present on PAS D is bromine-rich. The source is currently unknown, but bromine is used as a common fire-retardant material which is added to plastics, electronics and other consumer products.

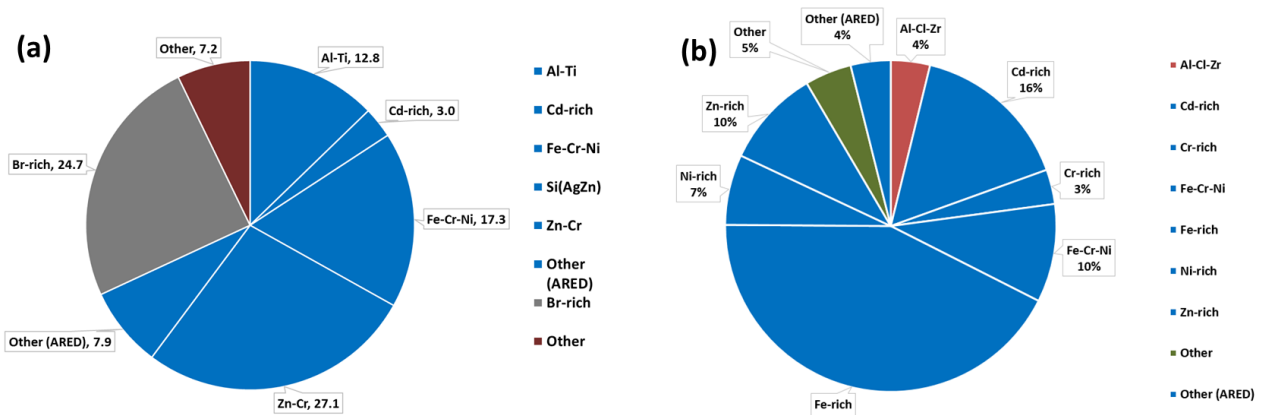


Figure 9. Percent concentrations of metal particles from CCSEM analysis, by weight, for two passive samplers in Node 3: (a) PAS D, day 16 substrate and (b) PAS G, day 8 substrate. The blue segments represent metals that are present in ARED, showing that a large proportion of the particles collected can be attributed to mechanical abrasion of moving parts of the exercise machine.

Fiberglass particles were observed on all passive sampler substrates. Fiberglass is easily recognizable by its morphology and EDS spectrum. The signature elements in fiberglass are aluminum, silicon and calcium, which

comprise a particle material class in the CCSEM analysis of carbonaceous particles in Figure 6. Fiberglass fibers are straight rods showing brittle fracture characteristics. Different sources of fiberglass may have different diameters. Figure 10 shows an example of fiberglass, in a bundle with carbonaceous platelets. Manual microscopy was performed on all the PAS montages to quantify the deposition of fiberglass in various locations. Almost all fiberglass fibers found were 8 μm in diameter. Plots in Figure 11 show that there are sources of fiberglass which are shedding uniformly, as linearly increasing quantities are evident on the substrates from days 2, 4, 8, 16 and 32. At the end of 32 days, Node 3 had the highest fiberglass populations (total 169 and 131 particles on PAS G and D, respectively) followed by Node 1 (119 particles on PAS B). The sources of fiberglass particles are not known at this time, but may be attributed to nonflammable cable sleeving. Larger diameter fiberglass fibers from a different source were found in very small quantities on PAS B, D, F and K.

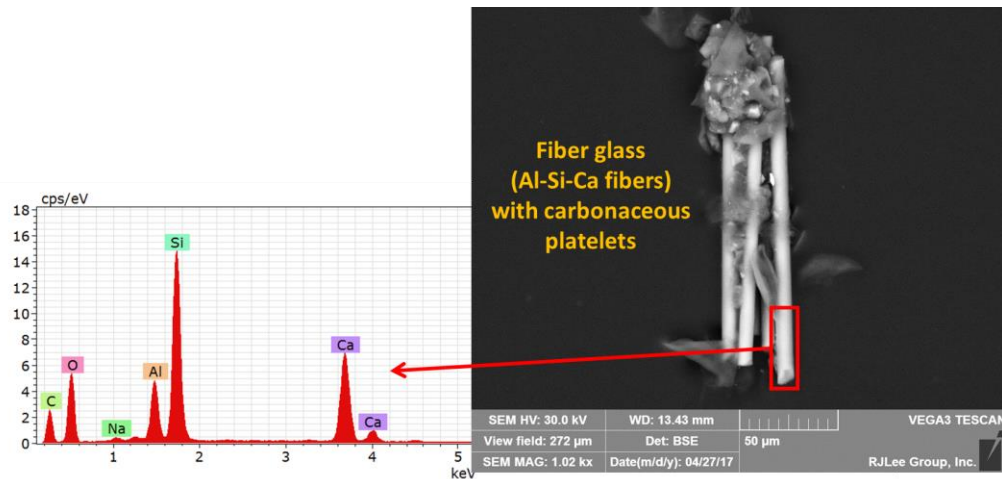


Figure 10. Example of a fiberglass bundle, recognizable by the signature elements aluminum, silicon and calcium, as well as the morphology of straight rods of equal diameter showing brittle fracture.

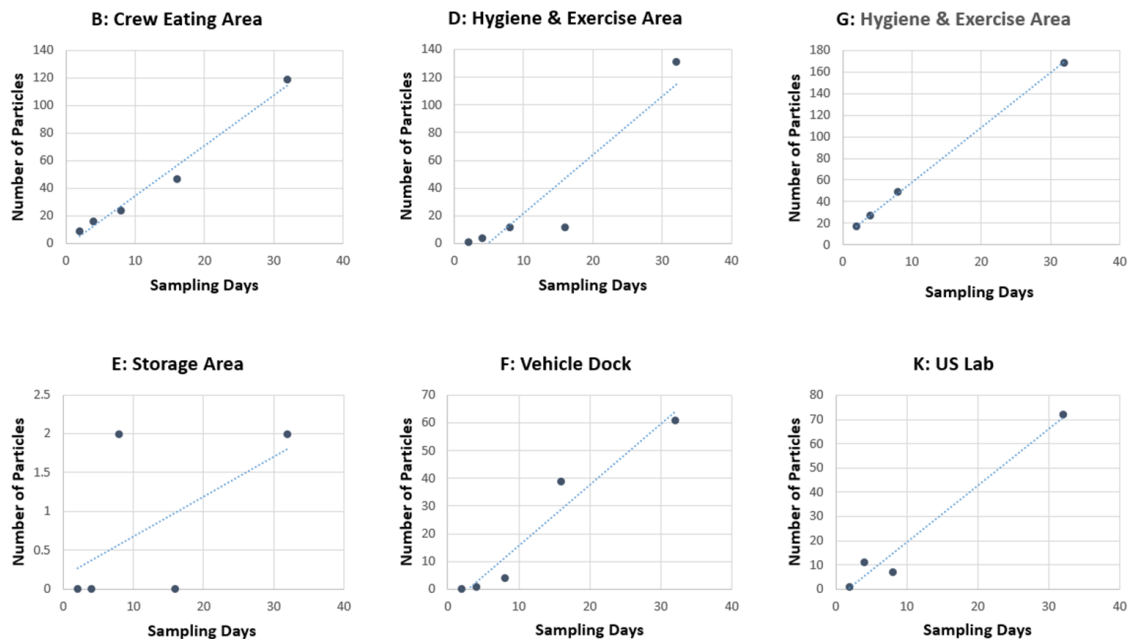
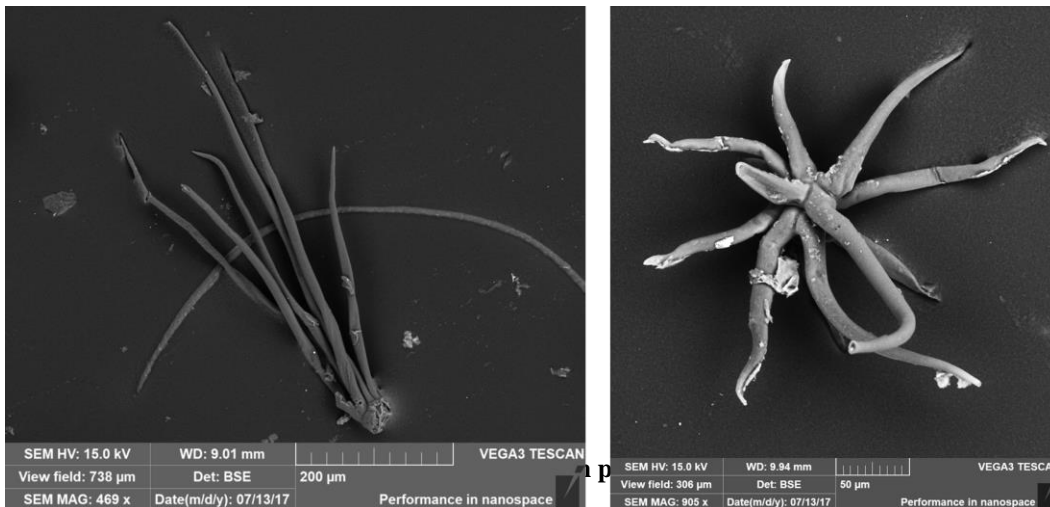


Figure 11. Fiberglass particle deposition over the 32 day sampling period in seven locations on ISS. Note that at the end of 32 days, Node 3 had the highest fiberglass populations (total 169 and 131 particles on PAS G and D, respectively) followed by Node 1 (119 particles on PAS B).

Assessing health effects of potential fiberglass inhalation by crew members is beyond the scope of this paper, however, it is widely accepted that these fibers are not as harmful as crystalline fibers such as asbestos. Fiberglass is classified as a synthetic vitreous fiber, and epidemiology studies show no strong evidence of harmful effects from inhalation, as fiberglass is cleared from the lungs relatively quickly.⁵



In surveying micrographs of carbonaceous particles, many seem to have morphology or patterns which indicate possible biological origins. One such particle type, thought to be trichomes, is shown in Figure 12. Trichomes are small plant hairs or appendages. These may have originated from a food source on ISS, or potentially from plant experiments. These trichomes were collected in Node 1 (left image) and the PMM (right image).

Additional source apportionment analyses on the passive samples are in progress. There is potential for this type of materials research to identify some particle emission sources that can be mitigated or reduced in future spacecraft environments. Some cannot be mitigated, but knowledge of particle emissions can influence future filtration system design, placement of exercise machines, and choice of materials in the equipment.

III. Active Sampler Results

Active sampling did not produce the abundance of data that passive sampling provided. On average, particle coverage was less than 1% of the grid area and the TEM grids were analyzed manually because the sparse particle coverage did not allow computer-controlled analyses. Unlike the passive samplers, which had multiple sample substrates at different exposure durations, the active sampler was limited to approximately six hours of sampling at the flow rate of 0.5 ml/min, based on the battery life of the sampler. The grids were analyzed in a Hitachi HD-2300 dedicated 200kV scanning transmission electron microscope (STEM) using Bright-field (BF), dark-field (DF) and secondary electron (SE) detectors to collect images. The size ranges of particles collected by the active sampler ranged from approximately 10 nm to several micrometers. The passive samplers cannot capture particles of this size because as the air flows towards the sampling substrate, these smallest particles remain entrained in the air and follow the velocity streamlines, flowing past the sticky carbon tape and into the filters. The active samplers were deployed in the same locations, within two feet of the passive samplers and sampled from the same air, but for a much shorter duration.

Titanium-rich particles were identified on all samples. Examples of titanium dioxide (TiO₂) particles are shown in Figure 13. Most are agglomerates with primary particle sizes ranging from 60 to 100 nm in diameter and total diameter ranging from approximately 150 nm to 600 nm (note that scale bars differ in these micrographs). Titanium dioxide, a bright white pigment, is ubiquitous in many consumer products.⁶ Possible sources of titanium dioxide particles on ISS are food, personal care products, clothing, paper, plastics, and paints.

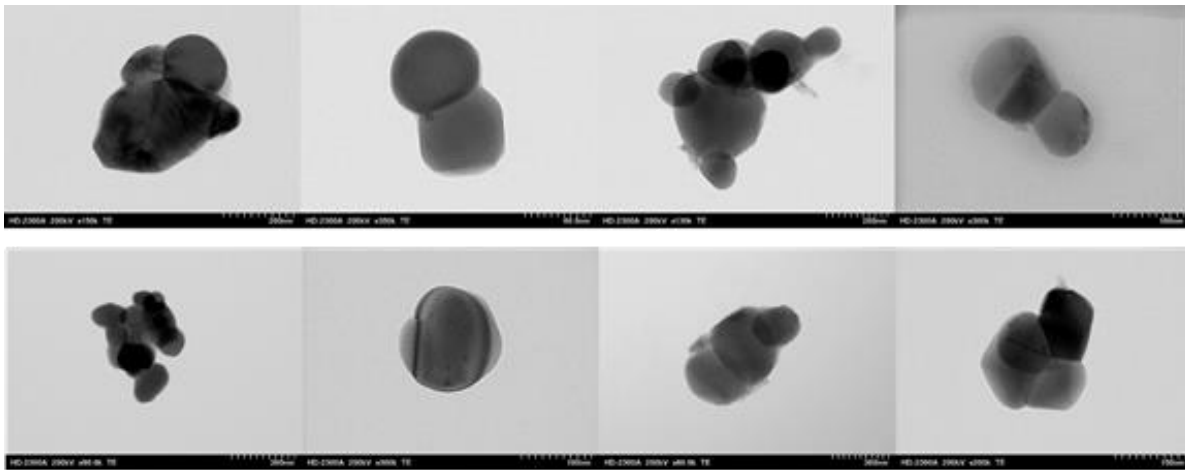


Figure 13. Examples of titanium dioxide (TiO_2) particles, which were found in all sampling locations. Most particles are agglomerates with primary particle sizes ranging from 60 to 100 nm in diameter. Note that scale bars differ in these micrographs, with agglomerate diameters ranging from ~150 nm to 600 nm.

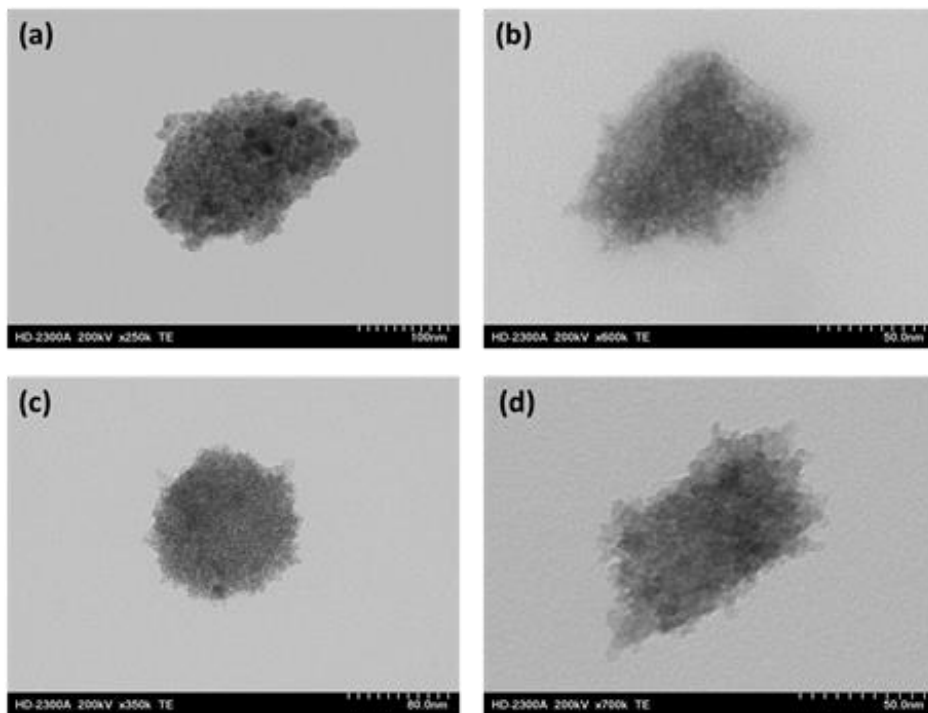


Figure 14. Examples of fume-like agglomerates, which were found in Node 3, the exercise and hygiene area. Primary particle sizes range from 3 to 20 nm in diameter. Particles (a) and (b) consist of iron and copper, particles (c) and (d) consist of iron and chromium. Note that the scale bars differ in these micrographs and agglomerate diameters range from approximately 50 nm to 200 nm.

Iron-containing fume-like particles (Fe/Cu, Fe/Cr, or Fe/Cu/Cr) were observed on most TEM grids. Unlike the mechanically generated metal particles on the passive samplers, the morphology of fume-like particles is more symmetrical, and consists of spherical primary particles that have been generated by a thermal process. When a metal is subjected to high enough temperatures it vaporizes. When the vapor cools, spherical nanoparticles are

formed by nucleation processes and subsequently grow by condensation. When present in high concentrations, the individual particles agglomerate, which reduces the number concentration and increases the average particle diameter significantly. Figure 14 shows examples of fume-like agglomerate particles, with primary particle sizes ranging from 3 to 20 nm in diameter and agglomerate diameters ranging from approximately 50 nm to 200 nm. The sources of these particles have not been identified, but the presence of these particles in every module (except the PMM storage area) indicates that there are multiple sources.

Other particle materials that were collected across multiple locations by the active samplers were sodium chloride (Na/Cl-rich particles), found in all locations except the PMM storage area; tin (Sn-rich particles), found in Nodes 2 and 3; and calcium or calcium/sulfur (Ca- and Ca/S-rich particles), in Nodes 2 and 3 and the US Lab.

IV. Future Work

The aerosol sampling experiment will be repeated in the re-flight of the sampling hardware in the summer of 2018. Emphasis will be placed on longer sampling durations for the active samplers. The current battery life is approximately 6 hours, so to lengthen sampling time, the battery must be recharged and the sampler replaced in the same location for a second day of sampling with the same TEM grid. The goal is to have adequate coverage of the TEM grid for automated microscopy and obtain better statistics on the smallest particle populations. Existing PAS montages can be further studied to identify more particle emission sources. Fiber analyses can quantify the hypothesis that lint from cotton clothing is the largest source of airborne fibers. Future passive samples will also provide a comparison of airborne pollutants collected 18 months apart.

V. Conclusion

The results of the Aerosol Sampling Experiment provided the first in-depth microscopic and materials analyses of airborne particulate matter on ISS, covering multiple locations. The variety and complexity of larger particles on the passive samplers is not surprising, given that the ISS has been continuously occupied by humans and is host to experiments and processes containing exotic materials, without any opportunity for dilution by ‘fresh air.’ Much can be learned from the aerosol sampling results. Identifying particle materials and emission sources on ISS is important to understand whether these aerosols have a significant impact on astronaut health. Many factors must be considered when assessing health effects of aerosol exposure, including particle composition, concentrations, and size.⁷ Another important outcome of sampling is assessing what types of particles must be measured in future particulate monitoring, and using the information to optimize instrument designs. All of these pursuits can improve the air quality on ISS and future spacecraft.

Acknowledgments

Funding for this study was provided by NASA Advanced Exploration Systems Life Support Systems Project. RJ Lee Group performed all microscopy under contract #NNX17EC75P. Additional contributions by NASA student interns Otto Jantarapet, Emily Blick and Joyce Tam are gratefully acknowledged.

References

- ¹Meyer, M., (2017) Aerosol Sampling Experiment on the International Space Station, 47th International Conference on Environmental Systems, ICES-2017-74, AIAA, Charleston, South Carolina, July 2017.
- ²Rasband, W.S., ImageJ, U. S. National Institutes of Health, Bethesda, Maryland, USA, <https://imagej.nih.gov/ij/>, 1997-2016.
- ³Loehr, J. A., Lee, S. M., English, K. L., Sibonga, J., Smith, S. M., Spiering, B. A., & Hagan, R. D. (2011). Musculoskeletal adaptations to training with the advanced resistive exercise device. *Medicine & Science in Sports & Exercise*, 43(1), 146-156.
- ⁴Selig, M., “Structural Analysis Report for the Advanced Resistive Exercise Device (ARED),” JSC 64219 Rev A, Systems Architecture and Integration Office Engineering Directorate, October 2008.
- ⁵Hesterberg, T.W., Hart, G.A., (2001) Synthetic vitreous fibers: a review of toxicology research and its impact on hazard classification, *Critical Reviews in Toxicology*, Vol. 31, 1.
- ⁶Weir, A., Westerhoff, P., Fabricius, L., Hristovski, K., & Von Goetz, N. (2012). Titanium dioxide nanoparticles in food and personal care products. *Environmental science & technology*, 46(4), 2242-2250.
- ⁷Davidson, C. I., Phalen, R. F., & Solomon, P. A. (2005). Airborne particulate matter and human health: a review. *Aerosol Science and Technology*, 39(8), 737-749.